Multimodal Biosensing for Vestibular Network-Based Cybersickness Detection

Gang Li, Mark McGill, Stephen Brewster, Chao Ping Chen, Joaquin A. Anguera, Adam Gazzaley, and Frank Pollick

***Abstract*—Virtual reality (VR) has the potential to induce cybersickness (CS), which impedes CS-susceptible VR users from the benefit of emerging VR applications. To better detect CS, the current study investigated whether/how the newly proposed human vestibular network (HVN) is involved in flagship consumer VR-induced CS by simultaneously recording autonomic physiological signals as well as neural signals generated in sensorimotor and cognitive domains. The VR stimuli were made up of one or two moderate CS-inducing entertaining task(s) as well as a mild CS-inducing cognitive task implemented before and after the moderate CS task(s). Results not only showed that CS impaired cognitive control ability, represented by the degree of attentional engagement, but also revealed that combined indicators from all three HVN domains could together establish the best regression relationship with CS ratings. More importantly, we found that every HVN domain had its unique advantage with the dynamic changes in CS severity and time. These results provide evidence for involvement of the HVN in CS and indicate the necessity of HVN-based CS detection.**

***Index Terms*—Virtual reality, cybersickness, multimodal sensing, cognitive control ability, vestibular network.**

Manuscript received May 11, 2021; revised September 25, 2021 and November 26, 2021; accepted December 5, 2021. Date of publication December 10, 2021; date of current version June 6, 2022. This work was supported in part by the European Research Council (ERC) through the European Union's Horizon 2020 Research and Innovation Programme under Grant 835197, and in part by the National Natural Science Foundation of China under Grant 61901264. *(Corresponding author: Frank Pollick.)*

Gang Li is with the Center for Social, Cognitive and Affective Neuroscience (cSCAN) in the School of Psychology and Neuroscience, University of Glasgow, G12 8QB Glasgow, U.K. and also with the School of Electronic Information and Electrical Engineering, Shanghai Jiao Tong University, Shanghai 200240, China (e-mail: gang.li@glasgow.ac.uk, lixiaogang110217@hotmail.com).

Mark McGill and Stephen Brewster are with the Glasgow Interactive Systems Section in the School of Computing Science, University of Glasgow, G12 8QQ Glasgow, U.K. (e-mail: mark.mcgill@glasgow.ac.uk; stephen.brewster@glasgow.ac.uk).

Chao Ping Chen is with the School of Electronic Information and Electrical Engineering, Shanghai Jiao Tong University, Shanghai 200240, China (e-mail: ccp@sjtu.edu.cn).

Joaquin. A. Anguera and Adam Gazzaley are with the Neuroscape Center in the Department of Neurology, University of California, San Francisco, CA 94158 USA (e-mail: joaquin.anguera@ucsf.edu; adam.gazzaley@ucsf.edu).

Frank Pollick is with the Center for Social, Cognitive and Affective Neuroscience (cSCAN) in the School of Psychology and Neuroscience, University of Glasgow, G12 8QB Glasgow, U.K. (e-mail: frank.pollick@glasgow.ac.uk).

Digital Object Identifier 10.1109/JBHI.2021.3134024

I. Introduction

THE term cybersickness (CS) was first used by McCauley & Sharkey in 1992 [1]. They delineated it as a special motion sickness (MS) that was triggered by visually-induced illusory self-motion, namely vection, in a virtual environment ("cyberspace"). The fundamental difference between CS and MS is that CS occurs strictly with pure visually-induced sickness without any real physical movements. In the context of consumer virtual reality (VR), many VR games that involve moving visual surroundings (e.g., tunnel travel, driving a vehicle or experiencing flight or rollercoasters) may elicit vection and trigger CS. Although a precise reason for the experience of CS is somewhat lacking, sensory-conflict theory (SCT) [2] is one proposal to explain the etiology of CS. That is, CS occurs when vection is not matched by corresponding vestibular information. To be more specific, there is an absence of actual responses from vestibular sensory organs: otoliths and/or semi-circular canals. These mismatched sensory inputs go through neural pathways arriving in the brain's multisensory information integration (MII) center, leading to a form of neurological confusion in the brain. This may result in autonomic symptoms, including cold sweating, nausea, oculomotor disturbances and disorientation [3]. This is why autonomic physiological signals are considered a straightforward way to detect CS [4]–[7].

fMRI studies show that the temporoparietal junction and parieto-insular vestibular cortex play an important role in the MII center [8] and also indicate an interesting interaction between the MII center and the cognitive domain [9]. Given these findings, a recent review article directly proposed that the function of the human vestibular system goes far beyond just the processing of information from two inner ear sensory organs. Instead, it is a widespread network (human vestibular network, HVN) that includes at least the autonomic, sensorimotor (which covers the MII center) and cognitive domains [10]. A collective view of these studies led us to hypothesize that the cognitive domain is involved in SCT. That is, SCT and the HVN seem to share three identical key brain domains; therefore, CS may be better detected using combined indicators of dynamic changes in the HVN instead of using autonomic physiological signals alone. However, direct evidence of the correlates of the HVN and CS is lacking.

Recent studies have replicated the methodology of vection induction used in previous fMRI studies and confirmed the involvement of the sensorimotor domain from the perspective of electroencephalography (EEG), such as significant change in

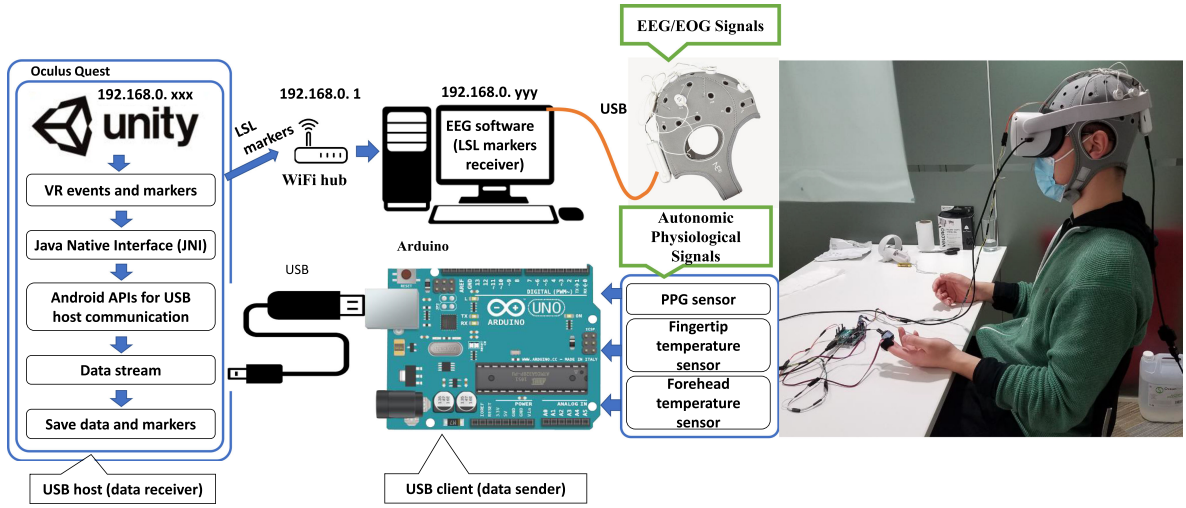

Fig. 1. (a) Block diagram of the proposed multimodal sensing system, where the Lab streaming layer (LSL) protocol was used to synchronize VR events with EEG data collection software. The LSL protocol, developed by University of California, San Diego a decade ago, can ensure sub-millisecond accuracy as long as both the LSL host (marker sender) and client (receiver) are in the same local network. The LSL's applicability in combined VR-EEG settings has been confirmed in our previous studies [25], [40]. For the physiological sensing platform, USB communication between Arduino and Oculus Quest was developed using middleware Java Native Interface (JNI) bindings. JNI was used to enable Java code to be called by a non-Java platform so that our VR application can access the hardware layer of Quest and stream all physiological data from Arduino's USB interface into quest and attach event markers to these data and directly store them as CSV files inside Quest. "Attaching event markers" was executed by two lines of consecutive C# code immediately after the task session started or after every 1-min FMS score reported. The latency was in the order of tens of milliseconds, so there were no meaningful system delays. (b) Sample experimental environment.

the Alpha frequency band in this domain during vection [11], [12]. However, it is still necessary to investigate other EEG frequency bands in a more comprehensive way because some traditional MS studies also observed significant changes in the Delta, Theta and Beta frequency bands [13], [14]. In a more recent study [15], Tauscher and colleagues investigated both EEG and autonomic physiological signals during CS using a physical projection room-based dome VR. The authors claimed that the reason they did not use a head mounted display (HMD) was that the straps on the HMD would interfere with the EEG signals. However, the latest flagship HMDs, such as the Oculus Quest 2, use EEG-friendly headbands (see Fig. 1) instead of cap-like straps. More importantly, although their EEG recordings covered cognitive and sensorimotor domains, they did not design the experiment and analyze data from the perspective of the HVN.

Regarding study design, previous studies have been mainly based on three steps [4]–[6], [16]: 1) baseline measurement prior to CS induction, 2) subjective ratings during CS induction using the fast motion sickness scale (FMS) [17] (if assessment during CS is the research topic) or the simulator sickness questionnaire (SSQ) [18] (if a pre-post CS comparison is the research focus), 3) validation of the effectiveness of the collected biodata by the subjective ratings. In the design of CS induction, issues such as serious symptoms (e.g., retching) have not been sufficiently considered, although they may affect the consistency between subjective and objective data [19]. For data validation, the SSQ is indeed frequently used in CS research; however, its two variants, CS questionnaire (CSQ) [20] and virtual reality sickness questionnaire (VRSQ) [21], appear to be superior to the SSQ for psychometric evaluation when using consumer VR HMDs [22]. More importantly, the cognitive domain has not been part of previous study designs; therefore, the correlation of cognitive indicators with subjective CS ratings remains unclear, as are interactions between cognitive and sensorimotor domains represented by EEG-based functional brain connectivity in CS. Therefore, the HVN as a whole is underexplored in CS detection.

Here, we aimed to understand how cognitive control abilities could be affected by CS and which biomarkers can best detect CS. Specifically, we assessed if moderate CS has a negative impact on some of the cognitive control indicators that are critical to work performance. As such, we designed an experimental procedure of cognitive task $\rightarrow$ moderate CS induction task(s) $\rightarrow$ cognitive task, where the cognitive task was a VR version of a previous cognitive assessment that featured low-vection visual elements and was used to assess selective attention-centric cognitive control abilities in the form of a perceptual discrimination task [23], [24], and the moderate CS induction task(s) were tunnel travel and a rollercoaster that featured high-vection scenes. Participants experienced high linear vection (tunnel task) with low rotational movement; stimuli that are expected to induce a moderate CS response. However, participants that did not reach our threshold of moderate CS response were subsequently exposed to a rollercoaster to experience high degrees of linear vection and also much greater amounts of circular vection. The benefit of this design was having a more robust CS induction strategy that is not detrimentally impacted by inherent population variability in subjective sickness ratings. We also conducted a control group experiment in which we repeated the experimental procedure described above, except with the moderate CS induction task(s) replaced by a vection-free neutral task.

We compared the differences between the first and second cognitive tasks in a set of well-established cognitive indicators.

Furthermore, because the cognitive task *per se* was VR-based and not zero-CS, we investigated the correlates of the cognitive indicators and CS ratings. More importantly, we took the HVN as a whole and explored the correlates of HVN-based biomarkers and CS ratings in all three conditions by simultaneously recording autonomic physiological signals [fingertip temperature, forehead temperature, heart rate (HR) and photoplethysmogram (PPG)-based heart rate variability (HRV)] and EEG signals generated in sensorimotor (temporoparietal junction and parieto-insular vestibular cortex) and cognitive domains (frontal to posterior midline), to explore which biomarkers are superior to others for the detection of CS and can thus be regulated to mitigate CS in future studies. Therefore, compared with previous studies, the primary contributions of this work are as follows:

1) This study linked EEG-based cognitive indicators and cognitive-sensorimotor functional connectivity indicators to subjective CS ratings, which can bridge the gap between the proposed HVN and a real-world case.
2) This study adopted multimodal biometrics so that neural and autonomic physiological data could be analyzed in the same framework.
3) This study built a theoretical foundation for the development of targeted interventions in real-world VR scenarios, where users might be switching between mild and strong vection tasks with some frequency over the course of the day.

II. System Architecture and Settings

Our sensing platform was based on the newly released all-in-one Oculus Quest 2 (72 Hz display refresh rate and 89° horizontal field of view). As shown in Fig. 1, it was equipped with continuous monitoring of multimodal signals [including EEG, electrooculogram (EOG), PPG, fingertip and forehead temperature] of the participant.

A. EEG for Cognitive and Sensorimotor Domains

EEG data were collected through an eight-channel EEG recording device (NE StarStim 8^{TM}, Neuroelectrics Inc, Barcelona, Spain), which uses a high-resolution, high-speed analog-to-digital converter (24 bit at 500 Hz sampling rate). Conventional wet electrodes were used and placed at seven channels, including locations used to infer the cognitive domain (Fz, Cz, and Pz) [23], temporoparietal junction, and the parieto-insular vestibular cortex-based sensorimotor domain (CP5, CP6, P3 and P4) [11], [25]–[27]. The remaining channel (EXT) was used to collect EOG using a disposable electrode on the left lower eyelid. The ground and reference electrodes were connected together and attached to the right earlobe using an ear clip. Note, that EEG is poor at measuring neural activity that occurs below the upper layers of the brain (the cortex); therefore, we used autonomic physiological signals as the best estimates of the neural activity related to the autonomic domain (believed to be located in subcortical areas, such as the amygdala [10]).

B. Autonomic Physiological Signals

PPG data were recorded from the fingertip of the left index finger using a set of reflective-type photoelectric sensors (including a light transmitter and receiver; https://pulsesensor.com/). HR and HRV were extracted and analyzed from continuous PPG signals [28], [29]. Fingertip temperature data were collected from the fingertip of the left middle finger using a digital thermometer (DS18B20, Maxim Integrated, Inc.). Forehead temperature data were collected from the participant's forehead skin using a non-contact infrared temperature sensor (MLX90614, Melexis, Inc.). The position of the forehead temperature sensor was just above the Quest 2's built-in proximity sensor. Both fingertip and forehead temperature sensors have a $\pm$ 0.5 °C measurement accuracy, which is acceptable in the context of up to 2–4 °C CS-induced difference [30].

III. Experimental Design and Analysis Methods

A. Questionnaires for Subjective CS Assessment

The SSQ has 16 items in total, including three specific symptom clusters: nausea (N), oculomotor (O), and disorientation (D). Nausea includes symptoms of the feeling of nausea, stomach awareness, increased salivation and burping. The oculomotor cluster includes eyestrain, difficulty focusing, blurred vision and headache and the disorientation cluster includes feelings of dizziness and vertigo. The total score (T) of the SSQ is the weighted sum of the three symptom cluster scores and is used to describe the overall severity.

Unlike the SSQ which is used to assess CS severity between pre-post CS induction, the FMS can rate CS severity quickly during CS induction (usually at 1-min intervals). Thus, the FMS has higher time resolution than the SSQ. However, the price paid for quicker assessment is that the FMS is a single item questionnaire that requires participants to focus on nausea, general discomfort, and stomach problems only to give an overall single score ranging from 0 (not at all) to 20 (severe). The VRSQ and the CSQ are two subsets of the original SSQ. VRSQ developers argued that with VR HMDs, nausea-related symptoms were not the principal components compared with oculomotor and disorientation components. Thus, they excluded SSQ-N items from the original 16 SSQ items and retained other SSQ-O and SSQ-D items. Regarding CSQ, the developer removed two vague symptoms from the original SSQ with the intention of more clearly indicating CS because some of the symptoms might be triggered by other causes, such as fatigue and sweating, which might occur due to pure physical effort over time. Remaining symptoms indicated two factors: dizziness and difficulty in focusing.

B. Experimental Procedure

Fig. 2 shows the procedure for the experimental group (viewable on YouTube: https://youtu.be/XHeSXcDID_0). For the control group, we repeated the same experimental procedure but with the moderate CS induction task(s) replaced by a vection-free neutral task (forest scene, which is viewable on YouTube: https://youtu.be/RwHr_6zmQW0). This forest scene

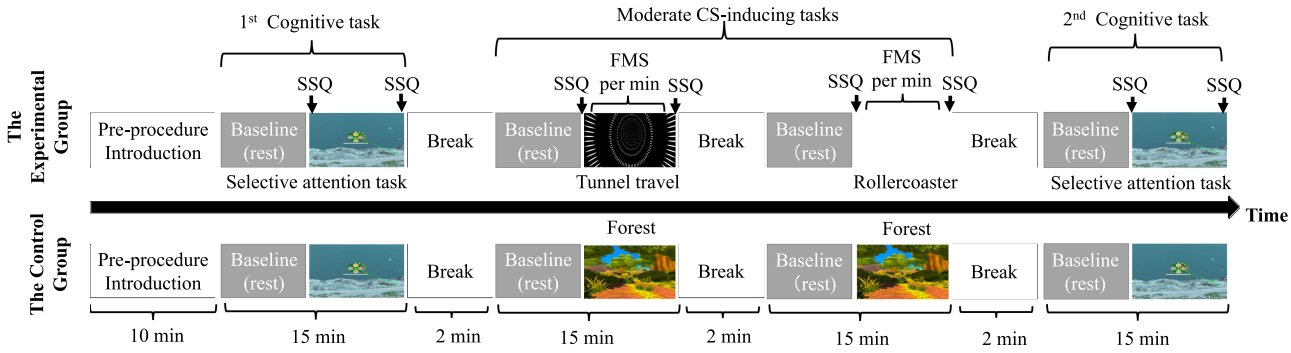

Fig. 2. Experimental design.

was 10-min long but implemented twice to match the maximum duration of the experimental group (e.g., tunnel travel + rollercoaster). This was a single-visit within-subject study including one pre-procedure introduction (during which a demo video was played on a laptop to minimize any pre-procedure anxiety) and three or four experimental blocks:

1) Mild CS-inducing cognitive task.
2) Moderate CS-inducing task 1 (tunnel travel).
3) Moderate CS-inducing task 2 [rollercoaster, not applicable if the participant had already dropped out or the FMS score had already exceeded the pre-defined threshold (FMS = 11) in the tunnel travel task].
4) Mild CS-inducing cognitive task.

Each block contained a 5-min baseline measurement prior to the 10-min VR task. During the baseline measurements, participants were required to close their eyes and listen to soft music (slow instrumental featuring traditional Chinese instruments). For each block, immediately after the baseline measurement and the task was completed, the participant was required to report SSQ scores (VRSQ and CSQ scores were calculated offline based on SSQ scores). Here, a digital version of the SSQ was directly implemented inside the VR scene so that participants could report their SSQ scores while wearing the VR headset by moving the virtual slider using the VR controller's thumbstick. Similarly, a digital version of the FMS was used to collect CS ratings at 1-min intervals. The purpose of using digital questionnaires was to minimize the opportunities for subjects to remove the VR headset, which could temporarily alleviate their symptoms and create a confound to the relationship between CS ratings and objective measures. The maximum FMS score is 20. Unlike the study of Lin et al. [19], which brought participants to the point of retching, to minimize the confounding effect of such symptomatic behavior and to comply with ethical requirements (that is, no more than moderate nausea symptoms), we stopped the experiment once the FMS score exceeded 11.

There were 2-min breaks between blocks. Apart from the breaks, participants wore the VR headset all the time and multimodal biodata were recorded throughout the whole experiment. CS symptoms may become severe as the exposure duration increases, particularly after using the VR device for 15 min [31], [32]; therefore, the multiple baselines and break time provided opportunities for us to induce CS but to avoid serious episodes of CS (e.g., deep breathing, swallowing and retching [19]), which was an ethical requirement. The procedure was approved by the ethics panel of the University of Glasgow (No. 300200009), College of Science and Engineering.

C. VR Tasks

Based on the experimental procedure, the following three VR tasks were all integrated into a single application (that is, a single .apk App file for Oculus Quest). This is a self-contained app; the experimenter did not need to perform any additional operation or verbally communicate with participants once the experiment started.

1) Cognitive Task: The cognitive task was a memory test that was adapted from Virtual Attention (VA), a novel VR HMD gaming platform developed at Neuroscape, University of California San Francisco [23]. The difference between the current version and that described in [23] is that we required participants to count and memorize the number of targets instead of pressing buttons to respond to the target. This was an attempt to minimize the confounding effect of physical effort, as suggested by the CSQ's developer. Each trial of the memory test begins with the appearance of a single ocean animal [either a "Target" (green sunfish) or a "Non-target" (a different colored sunfish or another ocean animal)]. The memory accuracy was calculated by dividing the total number of "Targets" by the counted number of "Targets". This task was designed as a mild vection VR stimulus; more vection occurred for those stimuli that moved in-depth compared with laterally moving objects [33], like the faint ripples of internal waves in the underwater environment.

2) Moderate CS Task (Tunnel Travel): As the name implies, the tunnel travel required the participant to travel in an abstract tunnel, mainly involving the perception of moving in-depth. This tunnel travel task was adapted from [34]. The route was set as a normal driving scenario, including curves, uphill and downhill paths, but without upside down and off-axis paths. Unlike the fixed movement speed in the original version of [34], the movement speed was adjustable in the present study. It was increased by 20% in the second time window if the same FMS score was reported in consecutive 2-min periods, in order to match the participant's different susceptibility threshold.

3) Moderate CS Task (Rollercoaster): Given that the vestibular sensory organs, otoliths and semi-circular canals, are sensitive to linear/gravity and angular acceleration stimuli, respectively [35], [36], the rollercoaster task aimed to cover both visual-otolith and visual-semi-circular canal mismatch through virtual linear and angular acceleration. Here, the virtual linear

TABLE I
SUMMARY OF THE OBJECTIVE METRICS USED IN THIS STUDY

HVN domains	Measurements		Implications
Cognitive (Fz, Cz, Pz)	Phase-locking values (PLVs) of inter-trial coherence (ITC) of frontal midline (Fz) at Theta band		The degree of attentional engagement
	Event-related spectrum perturbation (ERSP) of frontal midline (Fz) at Theta band		The initial attention level in cognitive discrimination
	Latency and amplitude of the event-related potential (ERP) at Fz (P3a)		The initial attention level in cognitive discrimination
	Latency and amplitude of the ERP at Pz (P3b)		The late-stage attention level in cognitive discrimination
	Beta/Theta ratio at Cz		Spontaneous EEG marker for attention level
	Relative band (Alpha) power (RBP*) at Cz		Spontaneous EEG marker for arousal level
Sensorimotor (CP5, P3, P4, CP6)	RBP (Theta~Beta) at all sites		Spontaneous EEG power spectrum at the four sensorimotor sites
	ERSP (Theta~Beta) at all sites		Event-related EEG power spectrum at the four sensorimotor sites
	PLVs of ITC (Theta~Beta) at all sites		The consistency of brain activities at the four sensorimotor sites
	PLVs of inter-electrode coherence (IEC) of (Theta~Beta) of right-to-left hemisphere		Brain functional connectivity between the right and left sensorimotor areas
Cognitive-Sensorimotor Interaction	PLVs of IEC of (Theta~Beta) in two directions: 1. Frontal midline (Fz) to right posterior (F2R for short); 2. Frontal midline (Fz) to left posterior (F2L for short); where the cluster of CP5 and P3 stands for left posterior and the cluster of CP6 and P4 stands for right posterior.		Brain functional connectivity between the cognitive domain and the right and left sensorimotor areas.
Autonomic	Heart Rate (HR)		Excitability of the autonomic nervous system
	Fingertip temperature (FT)		Thermoregulatory cutaneous responses
	Forehead temperature		Thermoregulatory cutaneous responses
	Heart rate variability (HRV)	LF/HF ratio**	Frequency domain feature for arousal level
		pNN-35***	Time domain feature for arousal level

*RBP was calculated by dividing the FFT power of one EEG band by the sum of the FFT power of all four EEG bands (δ, θ, α, and β). FFT power was calculated using a 1000-point Hanning (that is, a 2-s epoch since the EEG was sampled at 500 Hz) moving window with 500 (that is, 50%) overlapping points. **LF/HF ratio was calculated by dividing the FFT power of HRV's low frequency (LF) band (0.04–0.15 Hz) by the high frequency (HF) band (0.15–0.4 Hz). ***pNN-35 was the percentage of peak-to-peak intervals (>35 ms) divided by the total number of peak-to-peak intervals.

and angular stimuli were achieved by changing the speed of rotations and movements of a participant's point of view. Specifically, the participants' point of view was a camera that follows a programmable route that is created by placing a number of "waypoints" in the virtual space. When the camera passes through any of these waypoints, they can execute code that changes the rotation of the camera, the speed of these rotations, or the speed of movement of the camera through the route. Even though the route is restarted after roughly 1-min, the nature of the rotations leads to changes in the direction of the camera, making each lap slightly different than the rest, thereby avoiding predictability. Similar to tunnel travel, the movement speed of the rollercoaster was increased by 20% in the second time window if the same FMS score was reported in consecutive 2-min periods. This rollercoaster application has been shown to induce moderate CS symptoms in young adults in our previous study [37].

D. Data Pre-Processing and Feature Extractions

For EEG and EOG, a low-pass filter with a cutoff frequency of 40 Hz and a high-pass filter with a cutoff frequency of 0.1 Hz were applied to remove power line noise and DC drift, respectively. The filtered EEG data were then corrected using the mean of each channel and EOG-based independent component analysis. Regarding PPG, a band-pass filter (0.2 Hz–5.6 Hz) was used and then a 1st-order differential operation was used to remove the baseline wander (more details can be found in our previous study [28]). For temperature, we used the raw data without any pre-processing. Next, the metrics shown in Table I were extracted respectively for further analysis, where the definitions for EEG frequency bands were: Delta (0.1–3 Hz), Theta (4–7 Hz), Alpha (8–12 Hz) and Beta (13–20 Hz) [14]. The duration of the time window for extraction was 2000 ms (or −1000 to 1000 ms for event-related analysis) unless they were a standard window length, such as 1-min for HR and 5-min for HRV [38]. HRV metrics, LF/HF ratio [39], [40] and pNN-35 [41] were calculated using Kubios HRV Standard ver. 3.0 (commercial HRV analysis software https://www.kubios.com/). Other metrics were all calculated using custom MATLAB scripts and/or EEGLab v2020.0. (an open-source MATLAB plugin developed by Swartz Center for Computational Neuroscience; www.sccn.ucsd.edu/eeglab).

As shown in Table I, for the cognitive domain, the commonly-used metrics, such as event-related spectrum perturbation (ERSP)(Fz_{Theta}), phase-locking values (PLVs) of inter-trial coherence (ITC)(Fz_{Theta}), P3a, P3b and the Beta/Theta ratio at Cz, and relative band power (RBP)(Cz_{Alpha}) were extracted. These metrics were used in our previous VR studies to assess the attention level from different aspects [23], [42]. Among these, ERSP(Fz_{Theta}) and P3a were used to measure the initial

attentional processing. P3b was used to assess the late-stage of cognitive discrimination abilities. The PLV of ITC(Fz_{Theta}) was an indicator of the degree of attentional engagement (Min: 0; Max: 1). A value of 1 reflects perfect phase-locking across trials and a value of 0 reflects perfectly randomly distributed phases. Regarding the Beta/Theta ratio at Cz and RBP(Cz_{Alpha}), they are spontaneous EEG markers for attention [43] and arousal levels [44]. Except for P3a and P3b latencies and RBP(Cz_{Alpha}), higher values of these metrics were associated with higher levels of attention. For the sensorimotor domain, we explored a set of metrics in Delta $\sim$ Beta bands, including RBP, ERSP, PLVs of ITC and inter-electrode coherence (IEC), where the PLV of IEC was a measure to evaluate the functional connectivity from the perspective of EEG [45]. Particularly, we used the PLV of IEC to investigate if there was an interaction between the cognitive and sensorimotor domains. The PLV of IEC is calculated by cross-domain EEG electrode sites; therefore, it is a unique HVN biomarker.

E. Baseline Correction and Normalization

For SSQ-based analysis, all event-related potentials, and ERSP, ITC and IEC values were baseline-corrected using a -200 to 0 ms time period (thus, relative values were calculated for each participant to control individual state differences). Other metrics and SSQ, VRSQ and CSQ scores were normalized using the values in the baseline session of that block. For FMS-based analysis, we took the values in the first minute of that moderate CS induction task as the baseline, and then all metrics and FMS scores were normalized. The baseline-corrected and normalized data provided a means to normalize results so that the assessment of CS severity was not confounded by individual differences.

$$Normalized\ Metric = \frac{Raw - Baseline}{Baseline} \times 100\% \quad (1)$$

$$Normalized\ Score = \frac{Raw - Baseline}{Full\ Score} \times 100\% \quad (2)$$

Where, the full score used in (2) was to avoid division errors just in case the baseline score was zero. The values of the full score were determined according to their original publications [17], [18], [20], [21].

F. Statistical Analyses

The sickness ratings in the three time points were compared using a standard one-way repeated-measures ANOVA with time as the within-subject factor. This ANOVA analysis aimed to confirm whether the high-vection tunnel travel or rollercoaster induced more serious CS if compared with the low-vection cognitive tasks.

For the cognitive assessment, we used the paired t-test to compare differences between pre- and post- moderate CS induction in a set of well-established indicators of cognitive control abilities (see Table I), and for the behavioral measurement of memory accuracy. Regarding the correlates of HVN biomarkers and CS ratings at each time point per se, an automatic linear modeling (LINEAR) procedure with best subsets-based variable selection function [46], [47] in SPSS 19.0 was used for every HVN domain (that is, cognitive + sensorimotor + autonomic + IEC between cognitive and sensorimotor domains, as listed in Table I) to 1) investigate whether a statistically significant regression relationship existed, and 2) if so, to further investigate the most important and significant objective indicators and whether the combined indicators from every HVN domain could achieve better regression with higher adjusted R^2. For linear regression analyses, two sample cases per variable (called CS indicator in this study) tend to permit accurate estimation of regression coefficients [48]. The best subset-based regression would select a maximum 10 indicators each time to build the regression model; therefore, the required number of sample cases should be at least $10 \times 2 = 20$, which is consistent with our sample size of $N = 20$ for each group (see G. Participants). The number of indicators was different in each domain; therefore, we used Akaike's Information Criterion (AIC [49]–[51], the lower the better) as a reference to evaluate the performance of regression models. The statistical significance threshold was set as $p \leq 0.05$ for both regression model and indicators. Adjusted R^2 instead of R^2 was used as the metric to judge the performance of regression in the context of minimizing the overfitting problem. In SPSS, a leave-one-out method is used to compute the indicator importance (II), based on the sum of squared residuals (SSR) by removing one indicator at a time from the final full model (see (3)).

$$II = \frac{SSR\_without\_the\_indicator - SSR\_full\_model}{Sum\,(II)\_of\_all\_the\_indicators} \quad (3)$$

G. Participants

A total of 44 healthy right-handed young adults attended this study, 24 for the experimental group and 20 for the control group. Four participants in the experimental group were excluded onsite for the following reasons: 1) The PPG signals from three of them were abnormal because of very cold hands. 2) The data of one participant were unable to be normalized because his FMS score in the first minute had already exceeded the pre-defined threshold. Therefore, 40 participants (mean age: 23 y/o; range 20–32 years; 9 males) took part in the entire study. We focused on young people here because their cognitive functions are the most developed [45]. All participants had normal or corrected-to-normal vision, and were self-reported free from neurological/psychiatric disorders. All participants were required to sit still during each block. All participants reported playing less than 2 hr of video games per month. Also, all participants reported playing less than 30 min of VR games as of the experimental date. Therefore, there were neither professional game players nor first-time VR users [23]. All participants were paid £10/hr for their participation.

IV. Results

A. Subjective CS Ratings

One-way repeated ANOVA analysis shows that there were no statistically significant differences between the three time points in the control group for all nine kinds of sickness ratings

[that is, three questionnaires and their respective subscales: SSQ (×4), VRSQ (×3) and CSQ (×2)]; while there were statistically significant differences in most of the nine kinds of ratings [except for SSQ-O ($F(2,38) = 2.862$, $p = 0.007$] and CSQ-Diff [$F(2,38) = 0.997$), $p = 0.378$] in the experimental group. Further pairwise comparison results show that there were no significant differences between the two cognitive tasks, while there were significant differences in the comparisons of both the moderate CS task vs the 1st cognitive task and the moderate CS task vs the 2nd cognitive task for the majority of questionnaires. These results indicate that indeed high-vection tunnel travel or rollercoaster induced more serious CS compared with that induced by the low-vection cognitive task.

B. Cognitive Assessments

For the experimental group, paired t-test results showed that among the cognitive indicators in Table I, the degree of attentional engagement, and the initial attention level in cognitive discrimination, were decreased in the second cognitive task if compared with that in the first [$t(19) = 2.194$, $p = 0.041$ with the PLV of $ITC(Fz_{Theta}) = 0.198 \pm 0.007$ vs 0.181 ± 0.007 as well as $t(19) = 2.298$, $p = 0.033$ with $ERSP(Fz_{Theta}) = 0.178 \pm 0.078$ vs 0.021 ± 0.067 dB]; however, this decreasing trend of cognitive control abilities was not associated with a decreasing behavioral measurement [$t(19) = -0.34$, $p = 0.737$ with memory accuracy $= 98.2\% \pm 1.34$ and $98.7\% \pm 0.73$ for the first and second cognitive tasks, respectively]. These results indicate that the degree of attentional engagement and the initial attention level in cognitive discrimination were negatively affected by the moderate CS even though these effects had yet to lead to a significant difference in behavioral performance.

We repeated this analysis in the control group in which we found that the degree of attentional engagement and initial attention level in cognitive discrimination were increased in the second cognitive task [$t(19) = -8.255$, $p < 0.001$ with the PLV of $ITC(Fz_{Theta}) = 0.19 \pm 0.005$ vs 0.28 ± 0.009 as well as $t(19) = -4.105$, $p = 0.001$ with $ERSP(Fz_{Theta}) = -0.404 \pm 0.103$ vs 0.352 ± 0.135 dB] and were associated with an improved memory accuracy [$t(19) = -2.327$ with $90.843\% \pm 3.612$ vs $99.110\% \pm 0.633$]. This was a benefit of the control group because according to our previous study [23], a training effect (that is, improved performance) should be observed if the same cognitive task is carried out twice or more. Taken together, these results indicate that the moderate CS at least suppressed the training effect by reducing the participant's degree of attentional engagement and initial attention level in cognitive discrimination.

C. Exploring HVN-Based CS Biomarkers

As shown in Fig. 3, overall results showed that this brain network presented dynamic changes in CS severities with time. The cognitive domain was the predominant domain in the initial mild CS task, while the autonomic domain became the best one to describe CS during the moderate CS task performed later. Finally, when the same mild CS task was performed again, the sensorimotor domain stood out. We elaborate details of these results in the following three points.

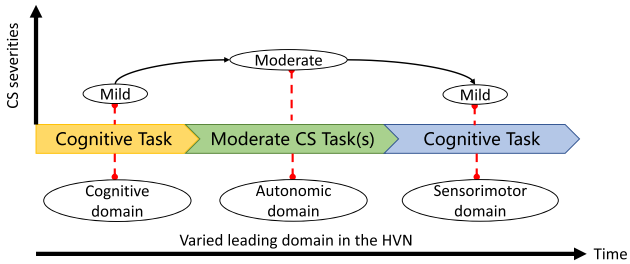

Fig. 3. Varied leading domain in the HVN.

1) The Cognitive Task (Pre-moderate CS): For the experimental group, Fig. 4(a) shows that both cognitive and sensorimotor indicators achieved eight significant regression relationships out of the nine kinds of CS ratings. The best regression relationship was achieved by combining the indicators of all three domains together for SSQ-D with adjusted $R^2 = 99.6\%$, $p < 0.001$ and $AIC = 29$. The importance ranking of the indicators in this best regression model showed the cognitive indicators, $ITC(Fz_{Theta})$ ($p < 0.001$, importance $= 0.227$) and $ERSP(Fz_{Theta})$ ($p < 0.001$, importance $= 0.196$), to be the top two (see Table II). Further regression coefficient analysis showed a negative relationship between $ITC(Fz_{Theta})$ and SSQ-D, but a positive relationship between $ERSP(Fz_{Theta})$ and P3b amplitude, indicating that as the symptoms of disorientation were worsening, the participant's degree of attentional engagement was decreasing while more attentional resources (no matter if it is for initial attentional processing or late-stage cognitive discrimination) were allocated. The reasoning behind the phenomenon of enhanced allocation of attentional resources is that the perception of vection per se is an attention-demanding cognitive activity [52].

In addition, we found that in this best model, Theta- and Beta-, together with the Alpha-related sensorimotor power spectrum indicators were selected, indicating the significance of investigating all EEG frequency bands in the sensorimotor area. More interestingly, we observed that three IEC indicators of midline frontal to left posterior areas [IEC(Delta), IEC(Alpha) and IEC(Beta)] were selected, indicating interaction between the frontal cognitive domain and the left sensorimotor domain. This result not only confirmed the existence of the cognitive-sensorimotor interaction but also further showed that it occurred in the left posterior sensorimotor area. This phenomenon was consistent with a previous neurostimulation study [27], in which the authors found that intervention on the left posterior sensorimotor area could mitigate traditional MS. We found that HR, the only selected autonomic indicator, ranked last. In the control group, the best model was achieved using SSQ-O and VRSQ-O. We found that $ITC(Fz_{Theta})$ was still ranked top ($p < 0.001$, importance $= 0.250$), followed by other sensorimotor and cognitive indicators. No autonomic indicators were selected. Taken together, these results clearly show that the leading domain of the HVN in the first cognitive task was cognitive, followed by sensorimotor and autonomic domains.

2) The Moderate CS Task: For the experimental group, Fig. 4(b) shows that the sensorimotor domain achieved significant regression relationships for all nine CS ratings, followed

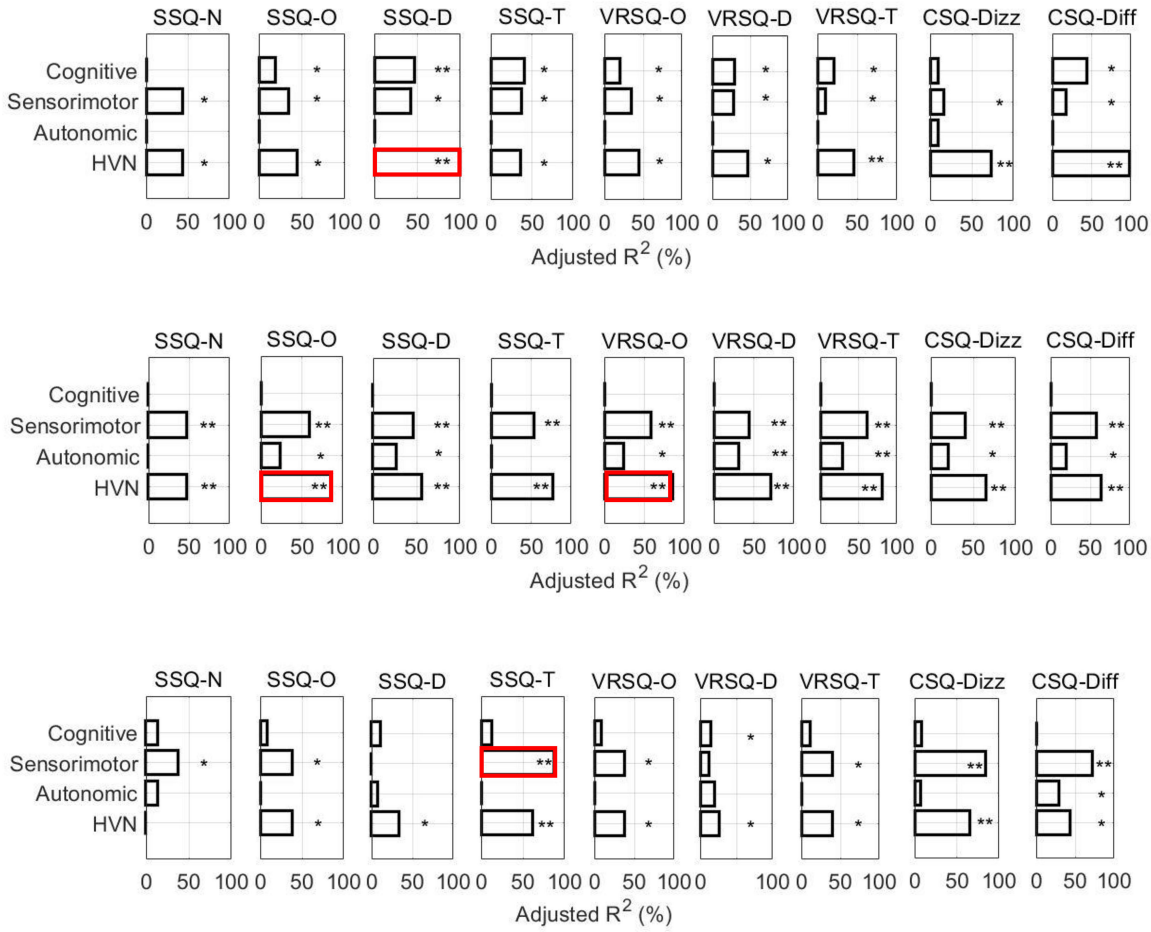

Fig. 4. The adjusted R^2 values of LINEAR analysis for every HVN domain and questionnaires. (a) The initial mild CS-inducing cognitive task. (b) The moderate CS-inducing tasks. (c) The 2nd mild CS-inducing cognitive task. $*p \leq 0.05$ $**p \leq 0.001$. The highest adjusted R^2 value in each task is marked in red. The label "HVN" stands for a set of combined biomarkers of cognitive + sensorimotor + automatic + IEC-based cognitive-to-sensorimotor functional connectivity.

TABLE II
RANKINGS OF THE SIGNIFICANT INDICATORS ($p \leq 0.05$) AND CORRESPONDING REGRESSION COEFFICIENTS

1st cognitive task			Moderate CS tasks			2nd cognitive task		
Indicators	Importance	Coefficient	Indicators	Importance	Coefficient	Indicators	Importance	Coefficient
$ITC(Fz_{Theta})$	0.227	-99.334	HR	0.102	0.473	$ITC(CP5_{Theta})$	0.267	-620.218
$ERSP(Fz_{Theta})$	0.196	23.056	Fingertip Temperature	0.089	2.210	$ERSP(CP5_{Beta})$	0.155	-30.667
$ERSP(CP5_{Theta})$	0.159	-16.628	$RBP(CP5_{Delta})$	0.085	1.921	$ERSP(P3_{Alpha})$	0.144	17.208
$P3b_{Amp}$	0.131	0.521	Facial Temperature	0.078	-5.415	$ERSP(P3_{Delta})$	0.115	15.022
$IEC(F2L_{Delta})$	0.063	-48.765	$RBP(CP5_{Alpha})$	0.077	0.734	$ITC(CP5_{Delta})$	0.113	216.322
$ERSP(P3_{Theta})$	0.050	8.524	$IEC(F2L_{Beta})$	0.073	-0.209	$ITC(CP6_{Alpha})$	0.079	216.764
$IEC(F2L_{Alpha})$	0.048	23.742	$ITC(P4_{Theta})$	0.073	-0.216	$ITC(P4_{Beta})$	0.074	213.788
$IEC(F2L_{Beta})$	0.044	30.066	$RBP(CP5_{Beta})$	0.073	0.366	$ERSP(CP6_{Alpha})$	0.054	7.723
$ERSP(CP5_{Beta})$	0.043	5.734	$RBP(CP5_{Theta})$	0.072	0.447			
HR	0.025	-0.564	$ITC(P3_{Theta})$	0.070	0.130			

by the autonomic domain in the context of SSQ-based analysis. We did not find any significant regressions for the cognitive domain. Similar to the first cognitive task, the best regression model was achieved using the indicators of all three domains with $R^2 = 85.4\%$, $p < 0.001$ and AIC = 119.29 for SSQ-O and VRSQ-O. Further analysis showed that ITC(Alpha) in the left sensorimotor area (P3) ($p < 0.001$, importance = 0.239) and facial temperature ($p < 0.001$, importance = 0.150) were the top two indicators. $ITC(P3_{Alpha})$ presented positive while facial temperature showed negative coefficients.

When we zoomed in the time resolution from SSQ-based 10-min to FMS-based 1-min, we found that the indicators of each

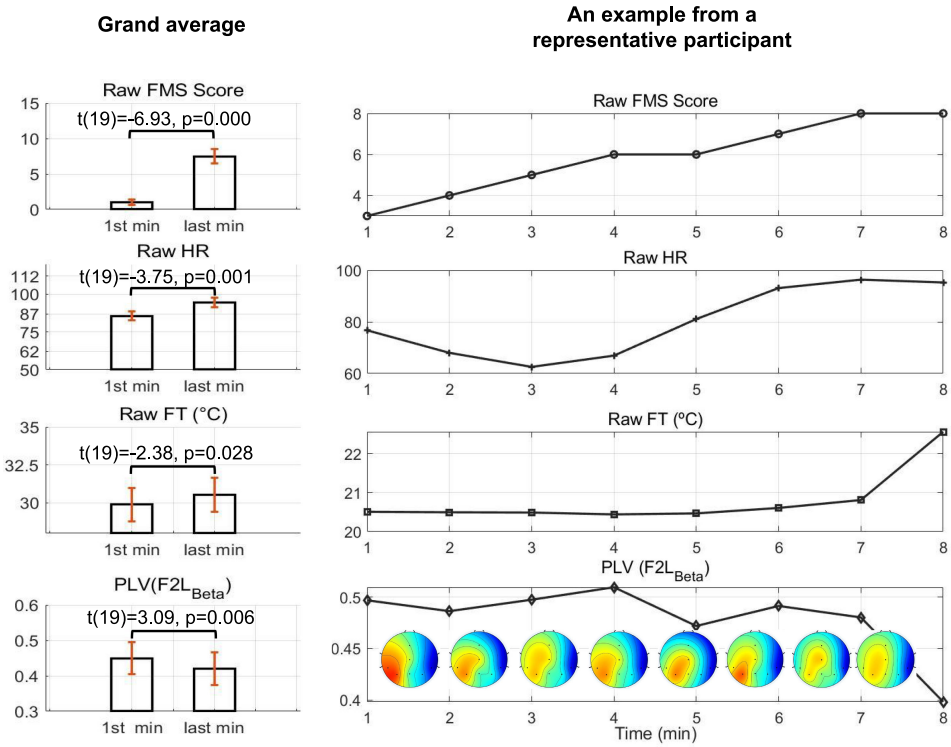

Fig. 5. Comparisons of the multimodal biodata in the first and last minute during moderate CS-inducing tasks. The grand average data is shown by the bar charts (the *p* values were obtained using the paired t-test). An example from a representative participant who required withdraw at the 8th minute of the tunnel travel task is shown by the curve graphs. PLV stands for phase locking value (Min:0; Max:1) for IEC. A value of 1 reflects perfect phase-locking across trials and a value of 0 reflects perfectly randomly distributed phases. FT and F2L$_{\mathrm{Beta}}$ stand for the fingertip temperature and frontal cognitive to left sensorimotor IEC at Beta frequency band, respectively.

domain achieved significant regression relationships. Among these, the autonomic domain stood out with adjusted $R^2 = 33\%$, $p < 0.001$ and AIC $= 1061.69$, followed by the sensorimotor domain with adjusted $R^2 = 22.4\%$, $p < 0.001$ and AIC $= 1099.47$, while the cognitive domain contributed the least to this regression relationship with adjusted $R^2 = 3.2\%$, $p = 0.006$ and AIC $= 1134.39$. Still, the best regression model was achieved by combining all three domains together with adjusted $R^2 = 53.4\%$, $p < 0.001$ and AIC $= 999.56$. Table II shows that HR and fingertip temperature (FT) are the top two indicators with a positive coefficient for both, indicating increased autonomic responses with increased CS ratings. This is consistent with previous studies [4], [30]. None of the cognitive indicators were selected in the best model. These results indicate that the cognitive domain was no longer predominant while the sensorimotor and autonomic domains were more activated compared with the previous cognitive task period. We also found that frontal to left posterior IEC(Beta) was selected in the FMS-based best regression model, indicating that the cognitive-sensorimotor interaction still existed and showed consistency in the location of interaction based on the findings in the previous cognitive task period (That is, the left sensorimotor area; see Fig. 5). In the control group, we did not find any significant regression relationship between HVN biomarkers and the CS ratings of the neutral task (forest scene). These results showed that the importance of HVN-based biomarkers in the moderate CS condition was autonomic > sensorimotor > cognitive, which is partly consistent with work of Tauscher et al., who showed that the autonomic physiological signals were superior to EEG signals [15].

3) The Cognitive Task (post-moderate CS): According to our previous study in which the time of self-reported full recovery from moderate CS symptoms was less than 5 min [37], we hypothesized that the cognitive domain could be back to being the predominant element in the second cognitive task after the end of moderate CS induction and the 7-min relaxation (2-min break plus 5-min eye-closed baseline session). Indeed, this hypothesis can be verified from the self-reported CS ratings (as explained in Results A). However, from the perspective of biometrics, the cognitive assessments in Results B already showed that a participant's degree of attentional engagement represented by ITC($\mathrm{Fz}_{\mathrm{Theta}}$) and the initial attention level in cognitive discrimination represented by ERSP($\mathrm{Fz}_{\mathrm{Theta}}$) were reduced by moderate CS, even though further regression analysis [see Fig. 4(c)] indicated a weak sign of post-moderate CS recovery in the cognitive domain, evidenced by one significant regression relationship out of the nine CS ratings (that is, $R^2 = 15.3\%$, $p = 0.05$ and AIC $= 104.95$ for VRSQ-D). The best regression model was achieved by the sensorimotor domain with $R^2 = 87.5\%$, $p < 0.001$ and AIC $= 86.75$ for SSQ-T, indicating the significance of objective measurements (that is, EEG-based sensorimotor indicators) on the evaluation of the aftereffect of moderate CS. Unsurprisingly, two sensorimotor indicators, ITC($\mathrm{CP5}_{\mathrm{Theta}}$) and ERSP($\mathrm{CP5}_{\mathrm{Beta}}$), were selected

as the top two indicators in the best model (see Table II). Further examination of coefficients showed that both indicators had a negative relationship with CS ratings, indicating an inhibition effect of CS on Theta and Beta bands of the left sensorimotor area, which once again showed the necessity of investigating other non-Alpha EEG frequency bands. We did not find any significant indicators in cognitive-sensorimotor interaction and the autonomic domain. Unlike the experimental group above, the dominant position of ITC(Fz_{Theta}) ($p < 0.001$, importance $= 0.265$) reoccurred in the control group, followed by autonomic and sensorimotor indicators. Taken together, these results indicate that ITC(Fz_{Theta}) was a reliable indicator to represent the moderate CS-induced impact on cognitive control abilities.

V. Discussion

A. The Significance for Real-World Applications

We found that the cognitive control ability represented by the degree of attentional engagement was decreased by CS in a visual selective attention-based cognitive task. This phenomenon was confirmed by comparing cognitive indicators before and after a moderate CS condition and was also observed during the mild CS-inducing cognitive task *per se*. These results indicate that experiencing CS can have immediate consequences beyond CS alone, for example, people will perform worse at attentionally demanding real-world activities, such as mentally demanding work. Our results also show that multimodal biosensing-based HVN biomarkers could best detect CS if compared with a single modality (e.g., using cognitive, sensorimotor, and autonomic modalities alone), indicating that HVN biomarker-guided CS regulation with the goal of improving cognitive control ability is a feasible solution to mitigate VR-induced CS. This is especially pertinent given that last year, just as COVID-19 was sweeping the world, the flagship consumer VR, Oculus Quest 2 was launched along with its "Infinite Office" promotional video [53]. This video offers a whole new possibility for people who are already working from home to port the PC/laptop-based work environment to VR, just as forward-thinking researchers have suggested [54]. This possible change gives VR more functions for work rather than just the stereotypical game/entertainment platform. In the post-COVID-19 era, we foresee more opportunities to use VR in daily life, such as during commuting. Researchers have already started to investigate how people could use VR in cars and airplanes during travel [55], [56]; an important area where people could directly benefit from CS-reduced VR applications.

B. Comparison With Prior Works About CS Detection

This is the first study using HVN-based multimodal biometrics to detect consumer VR-induced CS. Based on automatic linear modelling analysis, we found that the combined indicators from all HVN domains achieved the best detection result with the highest adjusted R^2 value and lowest AIC value. However, currently we have no way to directly compare this regression-based result with previous studies, as few of them shared adjusted R^2 {only one was found [4] and our study produced better results than those in [4] with better adjusted R^2 value for SSQ-T (77.5% vs 29.6%), SSQ-N (47.5% vs 10.1%), SSQ-O (85.4% vs 67.4%) and SSQ-D (55.6% vs 26.8%)} and no previous study provided AIC values. But, some meaningful qualitative comparisons still can be made for other aspects: 1) Ground truth: we found two studies that used the same ground truth, FMS with 1-min time resolution [6], [7], but other studies just asked the participants to self-report their scores if they felt CS [5], [16], [57]. Thus, the time window of CS ratings was randomized which could lead to data being missed according to our previous experience [37]. 2) Data reliability: some consumer EEG devices were used to collect EEG data [16], [58]. Even though these authors claimed that the signal quality was confirmed by the devices' built-in algorithms, it remains unknown how compatible the hard shells of consumer EEG devices are with EEG-VR settings (no figures of the actual experimental settings are stated in these studies). The present study used a research-class device. Its feasibility for use with EEG collection in consumer VR conditions has been validated in both event-related and spontaneous situations [23], [42]. More importantly, data reliability can be directly based upon well-established cognitive indicators [e.g., frontal midline ITC(Theta) and ERSP(Theta) were ranked the top two indicators in our initial cognitive task].

C. Relationship Between HVN Domains

There is an open question about the HVN. That is, what is the functional architecture of the HVN? [10]. Do cognitive and sensorimotor domains require autonomic functioning as a background condition, or can the three domains work independently? Although the present study is unable to answer this circuit-level question, at least from the perspective of CS detection, we observed that autonomic functioning was not the primary domain in the mild CS conditions. Also, although we indeed observed that the cognitive-sensorimotor functional connectivity metrics significantly associated with CS ratings, they did not stand out in any task condition, according to the indicator rankings. These results seem to suggest the independence of every HVN domain. However, we observed that the combined indicators from all three domains could together establish the best correlations with CS ratings, indicating the interaction of every HVN domain. Taken together, these results likely suggest that the functional architecture of the HVN can change dynamically in the context of CS.

D. The Significance of Using Various Questionnaires

Subjective questionnaires are important measures to estimate the ground truth of CS; therefore, the present study used three kinds of questionnaire to evaluate CS more accurately. The results indeed revealed the significance of using various questionnaires. For example, Fig. 4(b) shows that the VRSQ-T in some cases showed a better regression relationship than the commonly-used SSQ-T, evidenced by higher R^2 and smaller AIC values for the sensorimotor domain ($R^2 = 61.6\%$, $p = 0.000$ and AIC $= 132.84$ vs $R^2 = 53.4\%$, $p = 0.000$ and AIC $= 141.45$) and a significant p value for the autonomic domain ($R^2 = 29\%$, $p = 0.004$ and AIC $= 147.36$ vs $R^2 = 0\%$, $p = 1$ and

AIC = 159.39). In addition, non-SSQ questionnaires can show their uniqueness. For example, we would miss the opportunity to observe the sign of recovery in the cognitive domain and the CS aftereffect on the autonomic domain were we not using the VRSQ-D and CSQ-Diff. These empirical findings suggest that it is necessary to create and validate a larger composite questionnaire for future CS studies. This will provide a more robust estimation of the CS ground truth to provide as much subjective information as possible to interpret the objective biomarkers found.

E. Limitations

Although the present findings provide evidence demonstrating that indeed SCT and the HVN seem to share three brain domains in the context of consumer VR-induced CS, the nature of the experiment does not provide a mechanistic understanding of how SCT works on the HVN. To be specific, the causal evidence between CS and the HVN needs to be captured by further neurostimulation experiments that can directly manipulate the HVN metrics and CS ratings. For example, transcranial alternating current stimulation can be used to modulate the phase coherence between the cognitive and sensorimotor domain and to investigate if CS ratings are significantly associated with the modulation effects. In addition, the current study does not explore the functional architecture of the HVN and this needs to be addressed. Moreover, FMS is only a measurement of nausea and general discomfort during CS induction. Thus, the conclusion about the predominant position of the autonomic domain during CS induction may be different if other questionnaires are used. However, to our best knowledge, except for FMS, no questionnaires are currently regularly used to evaluate CS with a shorter time window. This study used two kinds of CS induction task to induce moderate CS. One was the tunnel travel, the other was the rollercoaster, which was a more nauseating version of the tunnel ride for people with higher susceptibility thresholds. The benefit of this kind of design was having a more robust (near-personalized) CS induction strategy that is not detrimentally impacted by inherent population variability during subjective sickness ratings. However, one problem of this approach is that it is not possible to research the two CS induction conditions respectively; therefore, the selected biomarkers in the FMS-HVN regression relationship can only be used to detect the CS grade, and may not identify the specific type of vection behind the CS. Also, the autonomic domain was represented by autonomic physiological signals; a more direct measurement should be performed once brain data from VR-fMRI settings become available in the future. Furthermore, the present study was conducted in right-handed healthy young adults. Further research is needed to explore how well the HVN links to CS ratings in different populations.

VI. Conclusion

The newly proposed HVN led us to hypothesize that CS may affect the cognitive domain. To verify this hypothesis, we designed an experimental procedure of cognitive task → moderate CS task(s) → cognitive task. We used the paired t-test to compare a set of well-established cognitive indicators with associated behavioral performance before and after participants experienced the induced moderate CS. We then employed a multiple regression method to put those cognitive indicators in the context of HVN-based biomarkers to investigate their correlations with CS ratings. The paired t-test results confirmed that indeed the cognitive control ability represented by the degree of attentional engagement was reduced by moderate CS and was behaviorally associated with a suppressed training effect. These results indicate that moderate CS may reduce the sustained attention abilities that are critical to work performance. Therefore, future studies can be designed to investigate the relationship between CS and sustained attention. Regression results revealed that single domain-based CS detection is not reliable. We should take the HVN as an indivisible whole to objectively detect CS, particularly in real-world daily VR applications where users might be switching between low and high vection tasks based on necessity, e.g., pausing work to engage in entertainment and then going back to work again.

Acknowledgment

A special thanks to Prof. Ian M. Thornton of the Department of Cognitive Science, University of Malta, for his help designing the tunnel travel task used in this study.

References

[1] M. McCauley and T. J. Sharkey, "Cybersickness: Perception of self-motion in virtual environments," *Presence Teleoperators Virtual Environ.,* vol. 3, no. 1, pp. 311–318, Aug. 1992.

[2] J. T. Reason, "Motion sickness—Some theoretical considerations," *Int. J. Man-Mach. Stud.*, vol. 1, no. 1, pp. 21–38, Jan. 1969.

[3] T. G. Dobie, "Symptoms and signs of motion sickness," in *Motion Sickness: A Motion Adaptation Syndrome,* 1st ed., vol. 6, N. I. Xiros, Ed., Cham, Switzerland: Springer, 2019, pp. 17–20.

[4] M. S. Dennison, A. Z. Wisti, and M. D'Zmura, "Use of physiological signals to predict cybersickness," *Displays*, vol. 44, pp. 42–52, Sep. 2016.

[5] R. Islam, Y. Lee, M. Jaloli, I. Muhammad, D. Zhu, and J. Quarles, "Automatic detection of cybersickness from physiological signal in a virtual roller coaster simulation," in *Proc. IEEE Conf. Virtual Reality 3D User Interfaces Abstr. Workshops*, 2020, pp. 648–649.

[6] N. Martin, N. Mathieu, N. Pallamin, M. Ragot, and D. J.-M., "Automatic recognition of virtual reality sickness based on physiological signals," presented at IBC 2018, Oct. 2018. [Online]. Available: https://www.ibc.org/automatic-recognition-of-virtual-reality-sickness-based-on-physiological-signals/3337.article

[7] R. Islam, Y. Lee, M. Jaloli, I. Muhammad, D. Zhu, P. Rad, Y. Huang, and J. Quarles, "Automatic detection and prediction of cybersickness severity using deep neural networks from user's physiological signals," in *Proc. IEEE Int. Symp. Mixed Augmented Reality*, 2020, pp. 400–411.

[8] S. M. Frank and M. W. Greenlee, "The parieto-insular vestibular cortex in humans: More than a single area?," *J. Neurophysiol.*, vol. 120, no. 3, pp. 1438–1450, Sep. 2018.

[9] S. M. Frank, L. Sun, L. Forster, P. U. Tse, and M. W. Greenlee, "Cross-modal attention effects in the vestibular cortex during attentive tracking of moving objects," *J. Neurosci. Off. J. Soc. Neurosci.*, vol. 36, no. 50, pp. 12720–12728, Nov. 2016.

[10] E. R. Ferrè and P. Haggard, "Vestibular cognition: State-of-the-art and future directions," *Cogn. Neuropsychol.*, vol. 37, no. 7/8, pp. 413–420, Mar. 2020.

[11] J. Dowsett, C. S. Herrmann, M. Dieterich, and P. C. J. Taylor, "Shift in lateralization during illusory self-motion: EEG responses to visual flicker at 10 Hz and frequency-specific modulation by tACS," *Eur. J. Neurosci.*, vol. 51, no. 7, pp. 1657–1675, 2020.

[12] S. Harquel, M. Guerraz, P.-A. Barraud, and C. Cian, "Modulation of alpha waves in sensorimotor cortical networks during self-motion perception evoked by different visual-vestibular conflicts," *J. Neurophysiol.*, vol. 123, no. 1, pp. 346–355, Jan. 2020.

[13] A. Koohestani, D. Nahavandi, H. Asadi, P. M. Kebria, A. Khosravi, R. Alizadehsani, and S. Nahavandi, "A knowledge discovery in motion sickness: A comprehensive literature review," *IEEE Access*, vol. 7, pp. 85755–85770, 2019.

[14] Y.-C. Chen, J.-R. Duann, S.-W. Chuang, C.-L. Lin, L.-W. Ko, T.-P. Jung, and C.-T. Lin, "Spatial and temporal EEG dynamics of motion sickness," *NeuroImage*, vol. 49, no. 3, pp. 2862–2870, Feb. 2010.

[15] J. Tauscher, A. Witt, S. Bosse, F. W. Schottky, S. G. Susana, and C. M. Magnor, "Exploring neural and peripheral physiological correlates of simulator sickness," *Comput. Animat. Virtual Worlds*, vol. 31, no. 4/5, Aug. 2020.

[16] C. Liao, S. Tai, R. Chen, and H. Hendry, "Using EEG and deep learning to predict motion sickness under wearing a virtual reality device," *IEEE Access*, vol. 8, pp. 126784–126796, 2020.

[17] B. Keshavarz and H. Hecht, "Validating an efficient method to quantify motion sickness," *Hum. Factors J. Hum. Factors Ergon. Soc.*, vol. 53, no. 4, pp. 415–426, Aug. 2011.

[18] R. S. Kennedy, N. E. Lane, K. S. Berbaum, and M. G. Lilienthal, "Simulator sickness questionnaire: An enhanced method for quantifying simulator sickness," *Int. J. Aviat. Psychol.*, vol. 3, no. 3, pp. 203–220, Jul. 1993.

[19] C.-L. Lin, T.-P. Jung, S.-W. Chuang, J.-R. Duann, C.-T. Lin, and T.-W. Chiu, "Self-adjustments may account for the contradictory correlations between HRV and motion-sickness severity," *Int. J. Psychophysiol.*, vol. 87, no. 1, pp. 70–80, Jan. 2013.

[20] W. Stone Iii, "Psychometric evaluation of the simulator sickness questionnaire as a measure of cybersickness," Ph.D. dissertation, Dept. Psychology, Iowa State Univ., Ames, IA, USA, 2017.

[21] H. K. Kim, J. Park, Y. Choi, and M. Choe, "Virtual reality sickness questionnaire (VRSQ): Motion sickness measurement index in a virtual reality environment," *Appl. Ergon.*, vol. 69, pp. 66–73, May 2018.

[22] V. Sevinc and M. I. Berkman, "Psychometric evaluation of simulator sickness questionnaire and its variants as a measure of cybersickness in consumer virtual environments," *Appl. Ergon.*, vol. 82, Jan. 2020, Art. no. 102958.

[23] G. Li, J. A. Anguera, S. V. Javed, M. A. Khan, G. Wang, and A. Gazzaley, "Enhanced attention using head-mounted virtual reality," *J. Cogn. Neurosci.*, vol. 32, no. 8, pp. 1438–1454, Aug. 2020.

[24] C. E. Rolle, J. A. Anguera, S. N. Skinner, B. Voytek, and A. Gazzaley, "Enhancing spatial attention and working memory in younger and older adults," *J. Cogn. Neurosci.*, vol. 29, no. 9, pp. 1483–1497, Sep. 2017.

[25] N. Takeuchi, T. Mori, Y. Suzukamo, and S.-I. Izumi, "Modulation of excitability in the temporoparietal junction relieves virtual reality sickness," *Cyberpsychol. Behav. Soc. Netw.*, vol. 21, no. 6, pp. 381–387, Jun. 2018.

[26] A. Kyriakareli, S. Cousins, V. E. Pettorossi, and A. M. Bronstein, "Effect of transcranial direct current stimulation on vestibular-ocular and vestibulo-perceptual thresholds," *NeuroRep.*, vol. 24, no. 14, pp. 808–812, Oct. 2013.

[27] Q. Arshad, N. Cerchiai, U. Goga, Y. Nigmatullina, R. E. Roberts, A. P. Casani, J. F. Golding, M. A. Gresty, and A. M. Bronstein, "Electrocortical therapy for motion sickness," *Neurology*, vol. 85, no. 14, pp. 1257–1259, Oct. 2015.

[28] G. Li and W.-Y. Chung, "Detection of driver drowsiness using wavelet analysis of heart rate variability and a support vector machine classifier," *Sensors*, vol. 13, no. 12, pp. 16494–16511, Dec. 2013.

[29] N. Pinheiro, R. Couceiro, J. Henriques, J. Muehlsteff, I. Quintal, L. Goncalves, and P. Carvalho, "Can PPG be used for HRV analysis?," in *Proc. 8th Annu. Int. Conf. IEEE Eng. Med. Biol. Soc.*, 2016, pp. 2945–2949.

[30] E. Nalivaiko, S. L. Davis, K. L. Blackmore, A. Vakulin, and K. V. Nesbitt, "Cybersickness provoked by head-mounted display affects cutaneous vascular tone, heart rate and reaction time," *Physiol. Behav.*, vol. 151, pp. 583–590, Nov. 2015.

[31] K. M. Stanney, K. S. Hale, I. Nahmens, and R. S. Kennedy, "What to expect from immersive virtual environment exposure: Influences of gender, body mass index, and past experience," *Hum. Factors*, vol. 45, no. 3, pp. 504–520, Sep. 2003.

[32] J. Munafo, M. Diedrick, and T. A. Stoffregen, "The virtual reality head-mounted display Oculus Rift induces motion sickness and is sexist in its effects," *Exp. Brain Res.*, vol. 235, no. 3, pp. 889–901, Mar. 2017.

[33] K. Pöhlmann, J. Föcker, P. Dickinson, A. Parke, and L. O'Hare, "The effect of motion direction and eccentricity on vection, VR sickness and head movements in virtual reality," *Multisensory Res.*, vol. 36, no. 4, pp. 623–662, Apr. 2021.

[34] F. Caniard, H. H. Bülthoff, and I. M. Thornton, "Action can amplify motion-induced illusory displacement," *Front. Hum. Neurosci.*, vol. 8, Jan. 2015, Art. no. 1058.

[35] M. Gallagher and E. R. Ferrè, "Cybersickness: A multisensory integration perspective," *Multisensory Res.,* vol. 31, no. 7, pp. 645–674, Jan. 2018.

[36] K. E. Cullen, "Vestibular processing during natural self-motion: Implications for perception and action," *Nat. Rev. Neurosci.*, vol. 20, no. 6, pp. 346–363, Jun. 2019.

[37] G. Li, F. Macia-Varela, A. Habib, Q. Zhang, M. McGill, S. Brewster, and F. Pollick, "Exploring the feasibility of mitigating VR-HMD-induced cybersickness using cathodal transcranial direct current stimulation," in *Proc. IEEE Int. Conf. Artif. Intell. Virtual Reality*, 2020, pp. 123–129.

[38] "Heart rate variability: standards of measurement, physiological interpretation and clinical use. Task force of the European society of cardiology and the North American society of pacing and electrophysiology," *Circulation*, vol. 93, no. 5, pp. 1043–1065, Mar. 1996.

[39] H. Chu, M.-H. Li, S.-H. Juan, and W.-Y. Chiou, "Effects of transcutaneous electrical nerve stimulation on motion sickness induced by rotary chair: A crossover study," *J. Altern. Complement. Med.*, vol. 18, no. 5, pp. 494–500, May 2012.

[40] H. Chu, M.-H. Li, Y.-C. Huang, and S.-Y. Lee, "Simultaneous transcutaneous electrical nerve stimulation mitigates simulator sickness symptoms in healthy adults: A crossover study," *BMC Complement. Altern. Med.*, vol. 13, no. 1, Dec. 2013, Art. no. 84.

[41] J. Faller, J. Cummings, S. Saproo, and P. Sajda, "Regulation of arousal via online neurofeedback improves human performance in a demanding sensory-motor task," *Proc. Natl. Acad. Sci,* vol. 116, no. 13, pp. 6482–6490, Mar. 2019.

[42] G. Li, S. Zhou, Z. Kong, and M. Guo, "Closed-loop attention restoration theory for virtual reality-based attentional engagement enhancement," *Sensors*, vol. 20, no. 8, Apr. 2020, Art. no. 2208.

[43] J. D. Kropotov, "A P3B component as index of engagement operation," in *Quantitative EEG, Event-Related Potentials and Neurotherapy*, 1st ed. Cambridge, MA, USA: Acad. Press, 2009, pp. 399–410.

[44] S. Koelstra, C. Muhl, M. Soleymani, J.-S. Lee, A. Yazdani, T. Ebrahimi, T. Pun, A. Nijholt, and I. Patras, "DEAP: A database for emotion analysis; Using physiological signals," *IEEE Trans. Affect. Comput.*, vol. 3, no. 1, pp. 18–31, Jan. 2012.

[45] J. A. Anguera, J. Boccanfuso, J. L. Rintoul, O. AI-Hashimi, F. Faraji, J. Janowich, E. Kong, Y. Larraburo, C. Rolle, E. Johnston, and A. Gazzaley, "Video game training enhances cognitive control in older adults," *Nature*, vol. 501, no. 7465, pp. 97–101, Sep. 2013.

[46] A. Miller, *Subset Selection in Regression*, 2nd ed., Boca Raton, FL, USA: CRC press, 2002.

[47] X. Yan and X. G. Su, *Linear Regression Analysis: Theory and Computing*. 1st ed., Singapore: World Scientific, 2009.

[48] P. C. Austin, and E. W. Steyerberg, "The number of subjects per variable required in linear regression analyses," *J. Clinepi.*, vol. 68, no. 6, pp. 627–636, Jun. 2015.

[49] C. M. Hurvich and C.-L. Tsai, "Regression and time series model selection in small samples," *Biometrika*, vol. 16, no. 2, pp. 297–307, Jun. 1989.

[50] H. Yang, "The case for being automatic: Introducing the automatic linear modeling (LINEAR) procedure in SPSS statistics," vol. 39, 2013, Art. no. 2. Accessed: Sep. 20, 2021. [Online]. Available: http://www.glmj.org/archives/articles/Yang_v39n2.pdf

[51] H. Akaike, "A new look at the statistical model identification," *IEEE Trans. Autom. Control*, vol. 19, no. 6, pp. 716–723, Dec. 1974.

[52] T. Seno, H. Ito, and S. Sunaga, "The object and background hypothesis for vection," *Vis. Res.*, vol. 49, no. 24, pp. 2973–2982, Dec. 2009.

[53] K. Melnick, "Oculus quest 2's 'Infinite office' lets you create your own virtual workspace," *VRScout*, Sep. 16, 2020. Accessed: Sep. 15, 2021. [Online]. Available: https://vrscout.com/news/oculus-quest-2-infinite-office-announced

[54] M. McGill, A. Kehoe, E. Freeman, and S. Brewster, "Expanding the bounds of seated virtual workspaces," *ACM Trans. Comput.-Hum. Interaction*, vol. 27, no. 3, pp. 1–40, Jun. 2020.

[55] M. McGill, A. Ng, and S. Brewster, "I am the passenger: How visual motion cues can influence sickness for in-car VR," in *Proc. Comput.-Hum. Interaction*, 2017, pp. 5655–5668.

[56] J. R. Williamson, M. McGill, and K. Outram, "PlaneVR: Social acceptability of virtual reality for airplane passengers," in *Proc. Comput.-Hum. Interaction*, 2019, pp. 1–14.

[57] J. Kim, W. Kim, H. Oh, S. Lee, and S. Lee, "A deep cybersickness predictor based on brain signal analysis for virtual reality contents," in *Proc. EEE/CVF Int. Conf. Comput. Vis.*, 2019, pp. 10579–10588.

[58] D. Jeong, S. Yoo, and J. Yun, "Cybersickness analysis with EEG using deep learning algorithms," in *Proc. IEEE Conf. Virtual Reality 3D User Interfaces*, 2019, pp. 827–835.